Three-dimensional processing of ultrafast CT sialography for parotid masses.

D H Szolar, R Groell, K Preidler, H Braun, M A Stiskal, H Stammberger and W P Dillon

AJNR Am J Neuroradiol 1995, 16 (9) 1889-1893
http://www.ajnr.org/content/16/9/1889

Three-dimensional Processing of Ultrafast CT Sialography for Parotid Masses

Dieter H. Szolar, Reinhard Groell, Klaus Preidler, Hannes Braun, M. Alfred Stiskal, Heinz Stammberger, and William P. Dillon

PURPOSE: To evaluate the diagnostic potential of three-dimensional image processing of ultrafast CT sialography in comparison with conventional CT sialography in patients with parotid masses. **METHODS:** In nine patients, CT sialography was done with three-dimensional image processing. The visibility of anatomic details and pathologic findings, derived from three-dimensional images, were graded numerically by three observers and compared with the findings obtained from conventional CT sialograms. Histopathologic specimens were obtained in all cases. **RESULTS:** Ultrafast CT images showed no motion artifact. Three-dimensional CT sialography offered significant improvement in demonstration of ductal anatomy (2.5 ± 0.2 versus 1.5 ± 0.1, respectively) and ductal pathology (2.6 ± 0.1 versus 1.1 ± 0.2, respectively) over conventional CT sialography. In two cases, the therapeutic regimen was altered substantially. **CONCLUSION:** Ultrafast CT three-dimensional sialography has the potential to allow more precise presurgical planning and contributes to the diagnosis and therapy planning of parotid masses, especially in patients in whom MR image quality is degraded by motion artifact.

Index terms: Salivary glands, computed tomography; Computed tomography, three-dimensional

AJNR Am J Neuroradiol 16:1889–1893, October 1995

Computed tomography (CT) and CT sialography have fallen out of favor for evaluation of patients with parotid masses since the introduction and widespread availability of magnetic resonance (MR) imaging (1–4). However, CT is still preferred to MR when there is a contraindication to MR imaging, in cases that require an increased confidence level in differential diagnosis, and for defining suspected bone involvement (5, 6). Additional contrast between neoplasms and surrounding parotid parenchyma can be achieved with CT after sialography (7–11).

Disadvantages of conventional CT sialography include the requirement for intravenous administration of atropine to minimize early runoff of contrast and impaired ductal opacification caused by prolonged scan time. This problem can be overcome with ultrafast CT imaging techniques. Moreover, three-dimensional imaging methods recently have gained increasing popularity and are helpful in reconstructive facial surgery, tumor staging, radiation planning, stereolithographic techniques, musculoskeletal imaging, and trauma (12–15).

We applied ultrafast CT sialography with 3-D image processing in patients with parotid masses to elucidate its diagnostic benefit over conventional CT sialography.

Subjects and Methods

Nine previously untreated patients (two female, seven male; mean age, 64 years; range, 35 to 86 years) with clinical evidence of a parotid mass, in whom MR image quality was degraded by motion artifact, underwent ultrafast CT (electron beam tomography CT; Siemens Evolution, Erlangen, Germany) of the parotid region. Before intraductal contrast administration, scans were performed at 130 kV and 620 mA · s with a single-section volume mode, to exclude intraglandular calcifications. Section

Received February 3, 1995; accepted after revision May 5, 1995.

From the Department of Radiology, University of California, San Francisco Medical School (D.H.S., M.A.S., W.P.D.); and the Departments of Radiology (R.G., K.P.) and Otolaryngology (H.B., H.S.), Kail-Frenzens Medical School, University Hospital Gray, Austria.

Address reprint requests to William P. Dillon, MD, Department of Radiology, Neuroradiology Section, University of California San Francisco, 505 Parnassus Ave, San Francisco, CA 94143-0628.

AJNR 16:1889–1893, Oct 1995 0195-6108/95/1609–1889

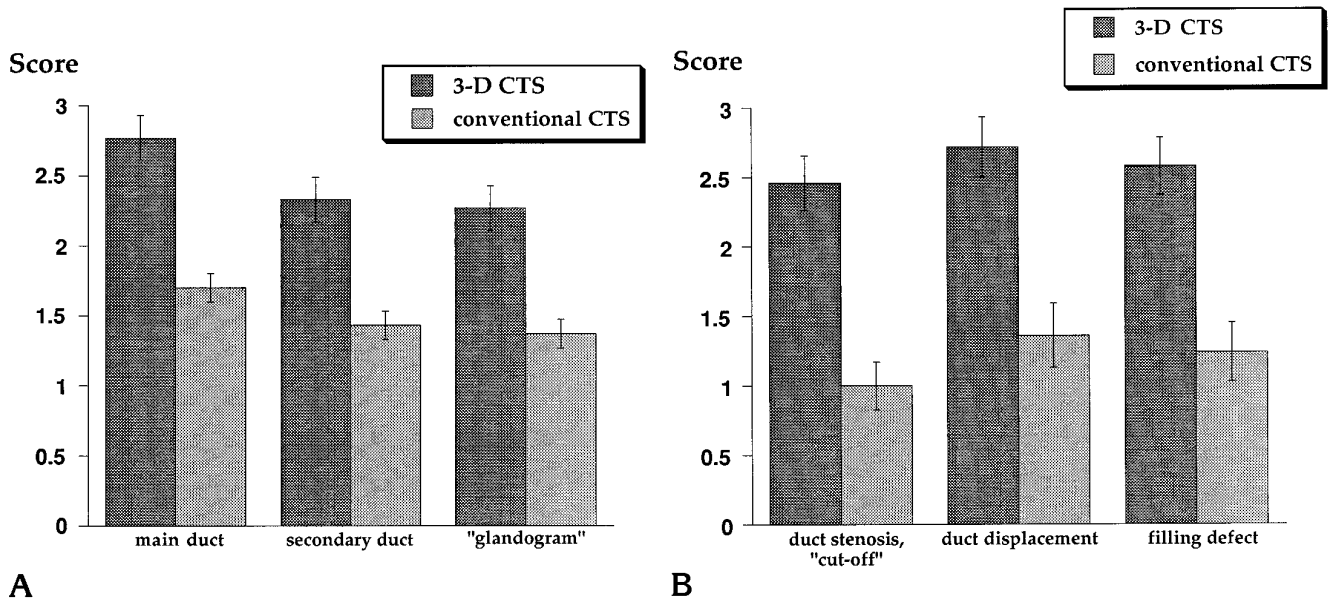

Fig 1. Qualitative results. Comparison of conventional and 3-D CT sialography (*CTS*) in demonstration of ductal anatomic detail (*A*) and ductal disease (*B*) (0 = no diagnostic information, 1 = poor, 2 = good, 3 = excellent).

thickness was 3 mm, and scan time per section was 0.3 seconds. Immediately after completion of this examination and after probing and dilation of the main parotid duct, 1 to 2 mL of water-soluble, nonionic contrast (Isovist 240; Schering, Berlin, Germany) was administered via a 30-cm, 3F (1.02-mm) sialography catheter (Portex Limited, Hythe, England). Scans were repeated at a section thickness of 1.5 mm in order to generate 3-D reconstructions of the parotid duct system. For 3-D surface reconstructions, the contrast-containing areas of the parotid gland were extracted at a threshold of 100 to 300 Hounsfield units, depending on the individual amount of contrast within the parotid duct system, and by using a single threshold method. The surrounding bone structures were extracted manually as necessary. The reconstruction matrix was 512^2 pixels. Surface presentations were obtained in five standard views (top, bottom, lateral, front, back) and additional oblique views oriented for optimal display of parotid duct anatomy. Scanning time per series was maximally 24 seconds.

Conventional CT and 3-D CT sialograms were assessed independently by three reviewers, using a numerical score system (0, no information; 1, poor; 2, good; 3, excellent information). Analysis of images entailed: (*a*) anatomic detail: main duct opacification, accessory duct visibility, and parenchymal structure, and (*b*) display of ductal disease: break-off sign, duct stenosis, duct displacement, parenchymal filling defect, and wall irregularities (signs of infiltration). Reviewers were blinded to the patient data. Average quality values and standard deviation were calculated. Differences between the scores of each modality were tested with a paired *t* test, and were considered significant when $P < .05$.

Histopathologic data were available in all cases. Patients underwent either surgery or biopsy.

Results

Ultrafast CT sialography caused no discomfort. Image quality of both conventional and 3-D-rendered CT sialograms was excellent in all cases, reflecting the absence of motion artifacts because of the fast imaging time. Histopathology proved five of the parotid masses to be malignant (squamous cell carcinoma, myoepithelial carcinoma, mucoepidermoid carcinoma, salivary duct carcinoma, and intraparotideal lymph node metastasis) and four benign (cystadenolymphoma [n = 2], pleomorphic adenoma, and chronic recurrent sialadenitis).

For demonstration of anatomic details, 3-D images were significantly superior to conventional images (2.46 ± 0.16 versus 1.50 ± 0.10, respectively) ($P < .05$). The quality of the main parotid duct was rated 3 in 85% of 3-D images and 20% of conventional images. 3-D rendering of images yielded a substantial improvement (Fig 1) in visibility of accessory ducts and display of the parotid's gland structure (glandogram).

The overall quality of display of ductal disease was significantly better on 3-D images than on conventional CT sialograms (2.59 ± 0.08 versus 1.28 ± 0.24, respectively) ($P <$

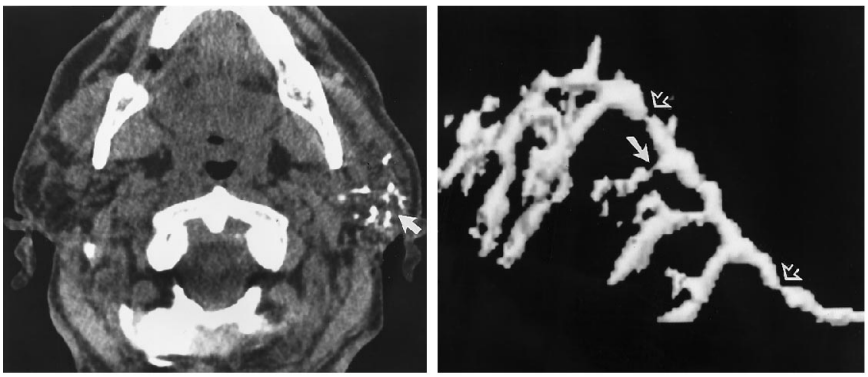

Fig 2. Chronic recurrent left parotid sialadenitis. *A*, Axial conventional CT scan after sialogram shows punctate accumulation of contrast material within presumed dilated intraparotid ducts (*arrow*). *B*, Three-dimensional CT sialogram (lateral view, left ductal system) shows focal areas of narrowing and prestenotic dilatation of both main (*open arrows*) and accessory ducts (*closed arrow*).

.05) (Fig 1). In one case with a histologically proven chronic recurrent sialadenitis, focal areas of narrowing of the main duct and accessory ducts were seen on 3-D images, increasing the confidence level for inflammatory parotid disease; conventional CT sialograms were unable to reveal this duct pattern (Fig 2). In another patient with a small salivary parotid duct carcinoma, 3-D reconstructions revealed a parenchymal filling defect and slight duct displacement, with break-off of secondary and tertiary ducts (Fig 3). Characteristic and common signs of a parotid mass, such as duct displacement and parenchymal filling defect, were seen more precisely on 3-D than on conventional CT sialograms. This provided useful adjunctive diagnostic information, and facilitated more accurate image interpretation (Figs 4 and 5).

Discussion

CT sialography was introduced in the late 1970s and early 1980s and has proven superior to noncontrast CT and sialography in showing small parotid masses and in differentiating between deep-lobe parotid tumors and parapharyngeal lesions (7–11). Nevertheless, numerous technique-related obstacles (early runoff of contrast caused by prolonged scanning time, intravenous administration of atropine to improve retention of contrast, and use of lipid-soluble contrast with relatively high side effects) and the advent of MR imaging particularly have led to the replacement of conventional CT sialography by MR as a preferable method in evaluating parotid masses.

Currently, the indications for this technique are fairly limited. The diagnostic workup of pa-

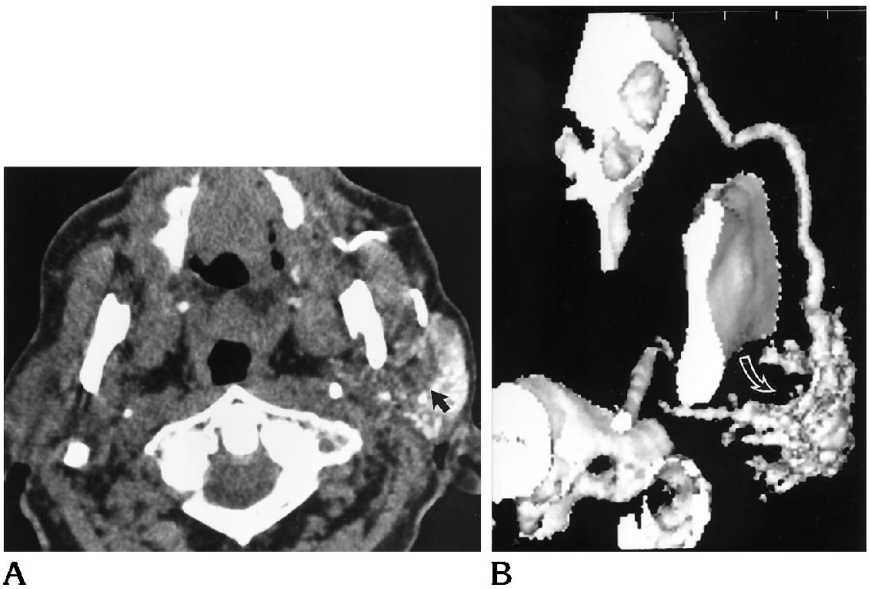

Fig 3. Small salivary duct carcinoma. *A*, Conventional CT scan after sialogram displays parenchymal filling defect (*arrow*), displacing the normal contrast-filled parotid gland. *B*, Three-dimensional rendering of CT sialogram (submental vertex view, left ductal system): the tumor displaces the normal parenchyma and duct. Break-off of accessory ducts is shown (*curved open arrow*). Note the excellent visibility of the normal main parotid duct.

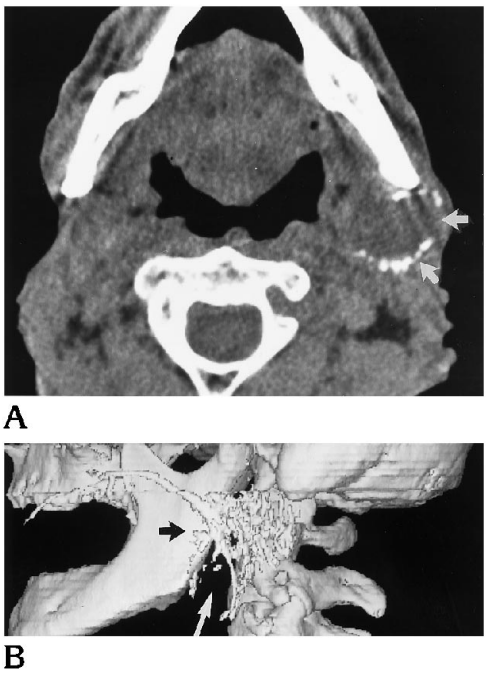

Fig 4. Cystadenolymphoma (Warthin tumor). *A*, Axial CT scan after sialography demonstrates displacement of the normal parotid parenchyma by tumor (*arrows*). *B*, Three-dimensional reconstruction (lateral view) shows the relationship of the tumor (*white arrow*), parotid tissue, and ductal system (*black arrow*).

tients with parotid masses should primarily consist of MR imaging or intravenously enhanced CT, in which almost all lesions can be detected. The application of CT sialography may be of use in those selected cases in which MR cannot be performed or is contraindicated, and a strong clinical suspicion of underlying disease exists but (*a*) the initial intravenously enhanced CT scan is negative or equivocal, or (*b*) there are diagnostic inconsistencies regarding the preoperative planning. Previous studies comparing conventional CT with CT sialography have indicated that CT sialography can provide more useful information than a routine noncontrast or contrast-enhanced CT, particularly in cases involving relatively dense parotid glands (16, 17).

In such circumstances, when CT sialography is performed for whatever reason, fast scanning combined with 3-D image processing offers improved display of anatomical detail. Neither premature runoff of contrast nor motion artifacts were observed in any patients. Even atraumatic fixation systems of the head, which recently have been proposed for 3-D reconstructions of the head to avoid movement, are not necessary (18). Three-dimensional rendering of the sialograms provided a substantial increase in visibility of normal anatomy and disease. In two cases, distinct pathologic features were seen only on 3-D images, which decisively influenced the surgical intervention.

More recently, Buckenham and associates (19), performing digital subtraction sialography in 109 patients with a variety of salivary gland diseases, stressed the advantages of improved image resolution and electronic manipulation

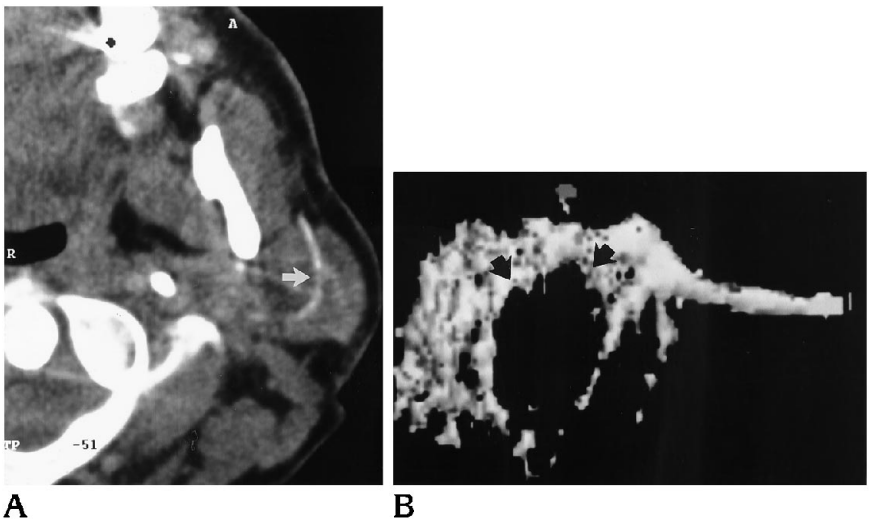

Fig 5. Pleomorphic adenoma. *A*, Axial CT scan reveals displacement of the main parotid duct by tumor (*arrow*), but only moderate contrast-filled parotid gland. *B*, Three-dimensional image (lateral display) shows marked splaying of the ductal system, duct displacement, and contrast-filling defect (*arrows*).

(magnification and dynamic review) of digital subtraction sialography over conventional sialography. However, digital subtraction sialography may have some limitations compared with ultrafast CT 3-D sialography, including the need to recannulate the duct orifice, the possibility of a higher radiation dose, and increased motion artifacts. However, further comparative studies between digital subtraction sialography and 3-D CT sialography would be needed to evaluate the diagnostic capability of both techniques with respect to image quality and demonstration of ductal morphology. Preliminary attempts to use MR sialography with an isoosmolally diluted MR contrast medium failed to show the parotid's duct system in five patients, as runoff of the contrast medium was noted before image acquisition in each patient (unpublished data).

In conclusion, 3-D CT sialography offers increased spatial resolution and improved image interpretation over routine CT sialography. More accurate delineation of anatomic detail and display of disease with respect to ductal anatomy allows more precise image interpretation, which can influence the therapeutic regimen. Even in cases in which conventional images were of equal value, the surgeons appreciated the spatial display of the parotid gland structures, which subjectively improved their impression of the anatomy. Because of the advantage of simultaneous assessment of the extent of both intraductal and extraductal parotid disease, future work may show that 3-D CT sialography can replace conventional sialography in some conditions. Present data suggest that 3-D rendering of the parotid ductal system might be helpful in detecting and characterizing the status of the ductal system in inflammatory processes of the parotid gland, such as autoimmune and chronic recurrent sialadenitis, and in evaluation of the glandular and periductal regions after trauma.

References

1. Tabor EK, Curtin HD. MR of salivary glands. *Radiol Clin North Am* 1989;27:379–392
2. Som PM, Biller HF. High-grade malignancies of the parotid gland: identification with MR imaging. *Radiology* 1989;173:823–826
3. Freling NJM, Molenaar WM, Vermey A, et al. Malignant parotid tumors: clinical use of MR imaging and histologic correlation. *Radiology* 1992;185:691–696
4. Weber AL. Imaging of the salivary glands. *Curr Opin Radiol* 1992; 4:117–122
5. Casselman JW, Mancuso AA. Major salivary gland masses: comparison of MR imaging and CT. *Radiology* 1987;165:183–189
6. Dillon WP, Mancuso AA. The oropharynx and nasopharynx. In: Newton TH, Hasso AN, Dillon WP, eds. *Computed Tomography of the Head and Neck*. New York: Raven Press, 1988:1–68
7. Mancuso AA, Rice D, Hanafee W. Computed tomography of the parotid gland during contrast sialography. *Radiology* 1979;132: 211–213
8. Som PM, Biller HF. The combined CT - sialogram. *Radiology* 1980;135:387–390
9. Stone DN, Mancuso AA, Rice D, Hanafee W. Parotid CT sialography. *Radiology* 1981;138:393–397
10. Carter BL, Karmody CS, Blickman JR, Panders AK. Computed tomography and sialography, I: normal anatomy. *J Comput Assist Tomogr* 1981;5:42–45
11. Carter BL, Karmody CS, Blickman JR, Panders AK. Computed tomography and sialography, II: pathology. *J Comput Assist Tomogr* 1981;5:46–53
12. Fishman E, Magid D, Ney D, et al. Three-dimensional imaging. *Radiology* 1991;181:321–327
13. Meglin AJ, Biedlingmaier JF, Mirvis SE. Three-dimensional computerized tomography in the evaluation of laryngeal injury. *Laryngoscope* 1991;101:202–207
14. Magid D, Fishman EK. Imaging of musculoskeletal trauma in three dimensions: an integrated 2-dimensional/3-dimensional approach with CT. *Radiol Clin North Am* 1989;27:783–789
15. Coia L, Galvin J, Sontag M, et al. Three-dimensional photon treatment planning in carcinomas of the larynx. *Int J Radiat Oncol Biol Phys* 1991;21:183–192
16. McGahan JP, Walter JP, Bernstein L. Evaluation of the parotid gland. *Radiology* 1984;152:453–458
17. Bryan RN, Miller RH, Ferreyro RI, et al. Computed tomography of the major salivary glands. *AJR Am J Roentgenol* 1982;139:547–554
18. Goerzer H, Heimberger K, Schindler E. Spiral CT angiography with digital subtraction of extra- and intracranial vessels. *J Comput Assist Tomogr* 1994;18:839–841
19. Buckenham TM, George CD, McVicar D, Moody AR, Coles GS. Digital subtraction sialography: imaging and intervention. *Br J Radiol* 1994;67:524–529